

## Software Development for Simulation of Reformer Furnace

**Zamaniyan, Akbar; Taghi Zoghi, Ali <sup>\*†</sup>**

*Gas Research Division, Research Institute of Petroleum Industry (RIPI), Tehran, I.R. IRAN*

**ABSTRACT:** In recent years, lots of research has been done on effective usage of natural gas; the first step in these processes is conversion of natural gas to Syngas. Natural gas reforming process by reformer furnace is commonly used for syngas and hydrogen production. In this paper, a windows based software, RIPI-RefSim, is introduced. By using proper heat, mass, kinetic and thermodynamic models as well as effect of catalyst shape, the software has been developed for the reformer furnace simulation for syngas and hydrogen production. RIPI-RefSim could be used in three different modes (Rating, Simulation and Design) and provides user a detailed understanding of furnace performance, product characteristics, temperature, reaction rates and pressure drop profiles, heat loss, effect of catalyst shape, and etc.

**KEY WORDS:** Terraced wall furnace, Methane-steam reforming, Software, Reformer, Furnace, Simulation, Modeling.

### INTRODUCTION

Steam reforming process is still one of the most economical routes for production of hydrogen and synthesis gas from natural gas. It generates synthesis gas for various purposes, such as ammonia and methanol production, OXO synthesis, iron ore reduction and various hydrocarbon production as well as hydrogen for hydrocracking and hydrotreating process. After desulfurization, the natural gas is mixed with steam and fed to the reforming furnace where chemical reactions take place in the presence of nickel containing catalyst. A mixture of CO, CO<sub>2</sub>, H<sub>2</sub>, unreacted CH<sub>4</sub> and steam leaves the reformer furnace. Four different furnace types are commonly used today (radiant wall, terraced wall, down fired and top fired types). The reformer reactors are

high performance furnaces, which contain 40 to 400 tubes. The internal tube diameter is commonly between 70 to 160 mm, with a tube wall thickness of 10 to 20 mm. The heated length is normally between 6 to 12 m depending on the furnace type. The tubes are made from high alloy nickel chromium steel (e.g. HK40: Cr 25%, Ni 20%, Co 4% or IN519: Cr 24%, Ni 24%, Nb 1.5%, Co 3%). The tubes are supported outside the furnace chamber either from the floor or the ceiling [1]. The reliability of the tubes is an important factor, because the failures can result in long down-periods for re-tubing and hence loss of production. Reactions take place at temperatures from 500 to 950 °C and pressures between 1500 and 3000 kPa. Reactor tubes are filled with nickel containing catalyst

*\* To whom correspondence should be addressed.*

*+ E-mail: Zoghiat@ripi.ir*

1021-9986/06/4/55

17/\$/3.70

pellets. Ni-Al<sub>2</sub>O<sub>3</sub> catalyst properties are dictated by severe operating conditions of high temperature and high steam partial pressure (close to 3000 kPa) [2].

From 1968 to now, the following various models have been developed for modeling of reformer reactors:

1- One dimensional homogeneous model (Hyman [3], Davies and Lihou [4], Golebiowski and Walas [5], Singh and Saraf [6]).

In this model reactor element has been considered homogen and mass transfer limitation eliminated. So this model can't be validated.

2- One dimensional heterogeneous model (Xu and Froment [7], Elnashaie et al. [8]).

In this model mass transfer limitation has been considered. This model is validate for reactor performance prediction in on dimension (axial direction).

3- Two dimensional heterogeneous model (Ferreira et al. [9], Pedernera et al. [10]).

This model has been developed for reactor performance prediction in axial and radial direction. The mass transfer limitation has been considered too.

In this work, one dimensional heterogeneous model because of good accuracy for industrial application, has been developed for reactor side and linked to furnace side model. Then a windows based software has been developed for simulation of industrial terraced wall reformer furnace. Terraced wall arrangement is one of the most common arrangements for methane-steam reforming reactor furnaces. The heat transfer model of terraced wall furnace (in furnace and tubes) has been coupled with chemical reaction, mass transfer and pressure drop models to predict the behavior of an industrial steam-reforming reactor [11]. The effect of catalyst pellet shape on the performance of the catalyst and steam reforming reactor have been considered too.

## REACTOR MATHEMATICAL MODEL

Fig. 1 shows a schematic diagram of the terraced wall reactor. Rows of vertical reaction tubes packed with Ni based reforming catalyst are installed in the furnace. Rows of burners in contact with the furnace walls supply the required heat for the endothermic reactions. Reactor feed which mainly consist of methane and reforming agents (steam and CO<sub>2</sub>) enters to the top of reactor tubes. To model the heat transfer in the furnace; furnace wall, tube skin, process gas and combustion gases are divided

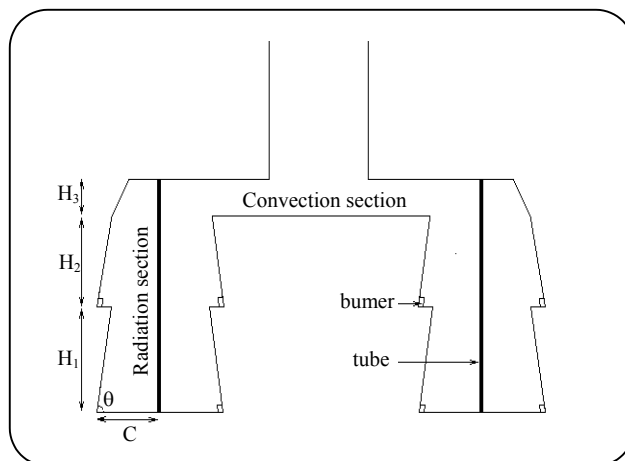


Fig. 1.: Schematic diagram of a terraced wall methane-steam reforming furnace.

into different zones and in each zone the heat transfer governing equations are set-up. Establishing the energy balances for the four types of heat transfer zones, a set of simultaneous nonlinear equations are obtained. Solving the set of nonlinear equations by iterative Newton method, the temperature distribution on the furnace walls, tubes skin, reaction gas inside the tubes and the combustion gas in the furnace are obtained [7, 12, 13].

The following methods have been developed for modelling of heat transfer behavior in furnaces:

- 1- Well stirred combustion chamber
- 2- Long furnace
- 3- Zone method
- 4- Monte carlo
- 5- CFD method (Computational Fluid Dynamic)

To simplify the complex and coupled phenomena of heat transfer and reaction into a mathematical model, a number of simplifying assumptions are considered. These assumptions provide a tractable model without sacrificing the accuracy. The major assumptions are:

- 1- Because of the large number of burners, high momentum of the combustion gases and good mixing in the furnace, the temperature and chemical composition of the combustion gases in the furnace is uniform.
- 2- Combustion gases, furnace wall and reaction tubes are gray bodies.
- 3- Elements of the furnace wall and reaction tubes are isothermal.

Considering the above generally acceptable assumptions, the governing equations of different heat transfer zones are established.

Fig. 2 shows a burner and the associated furnace wall. With all the heat transfer components into the element (m,n) an energy balance dictates that (see Fig. 3):

$$\left( \begin{array}{c} \text{Conduction} \\ \text{from neighboring} \\ \text{elements} \end{array} \right) + \left( \begin{array}{c} \text{Convection} \\ \text{from combustion} \\ \text{gases} \end{array} \right) + \quad (1)$$

$$\left( \begin{array}{c} \text{Radiation from all} \\ \text{the elements of tube} \\ \text{and combustion gases} \end{array} \right) + \left( \begin{array}{c} \text{Heat lost} \\ \text{to the} \\ \text{surroundings} \end{array} \right) = 0$$

That is:

$$(q_{m1,n} + q_{m,n+1} + q_{m+1,n} + q_{m,n-1}) + q_{\text{conv}} + (q_R + q_{g-1}) + q_{\text{lost}} = 0 \quad (2)$$

$$q_{g-1} = \left( \frac{\varepsilon_r + 1}{2} \right) \Delta x \Delta y (\varepsilon_g \sigma T_g^4 - \alpha_g \sigma T_{m,n}^4) \quad (3)$$

The conduction, convection and heat loss terms were derived from basic heat transfer equations. Convective heat transfer coefficients inside and outside the furnace were predicted by using empirical correlations [14]. The radiation terms were derived by an electric analogy and the shape factors were determined using the Cartesian coordinates of all the furnace wall and tube skin elements.

Fig. 4 shows the electric analogy of an element of the furnace wall, for which:

$$q_R = \frac{J_1 - E_{b1}}{R_1} \quad (4)$$

$$J_1 = \left( \frac{E_{b1}}{R_1} + \sum_{n=1}^{n=IT} \frac{E_{b2,n}}{R_{2,n} + R_{3,n}} \right) / AD \quad (5)$$

$$AD = \frac{1}{R_1} + \sum_{n=1}^{n=IT} \frac{1}{R_{2,n} + R_{3,n}}$$

IT is the number of elements of the tubes. The resistances and emissive powers are [15]:

$$R_1 = \frac{1 - \varepsilon_r}{A_1 \cdot \varepsilon_r} \quad (6)$$

$$R_2 = \frac{1}{A_1 \cdot F_{12} \cdot (1 - \alpha_g)} \quad (7)$$

$$R_3 = \frac{1 - \varepsilon_w}{A_2 \varepsilon_w} \quad (8)$$

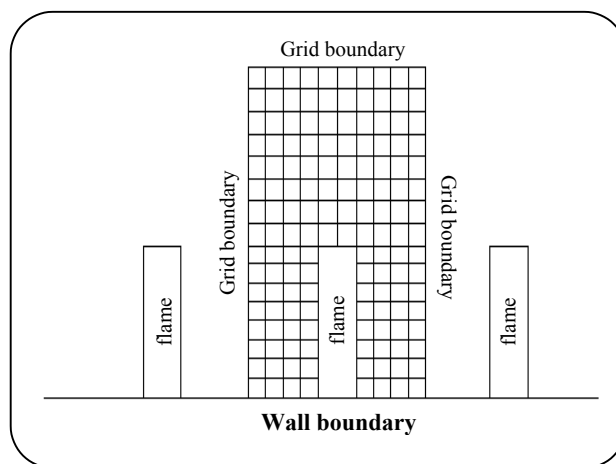


Fig. 2: Schematic diagram of a section of furnace wall and burners.

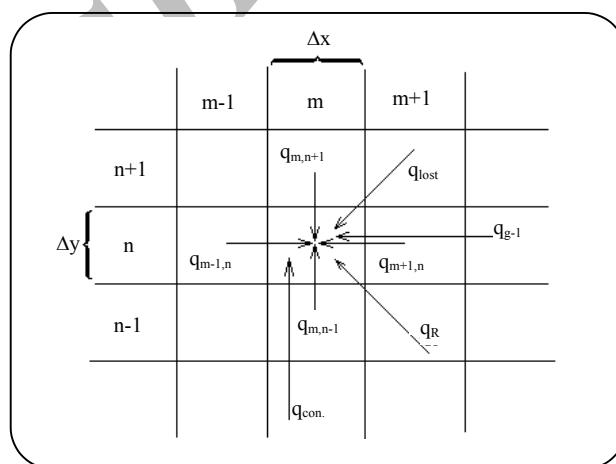


Fig. 3: An element of furnace wall.

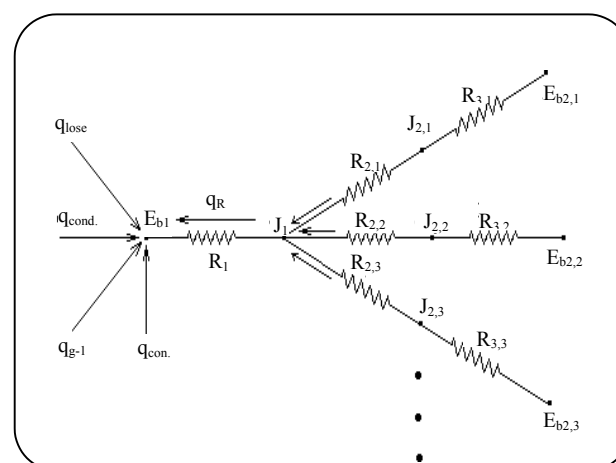


Fig. 4: Electric analogy of an element of furnace wall.

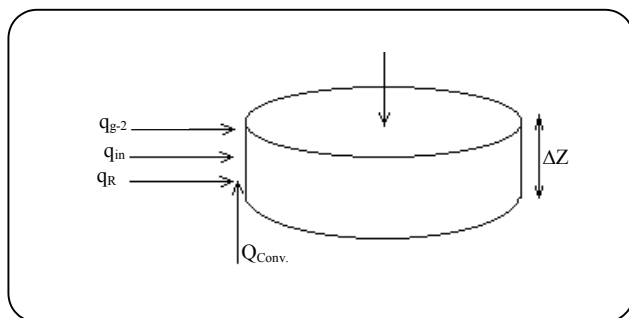


Fig. 5: Schematic diagram of an element of tube.

$$E_{b1} = \sigma T_{m,n}^4 \quad (9)$$

$$E_{b2} = \sigma T_w^4$$

Using the correlations for the flame height, the actual dimension of the burner flame has been taken into account. A correlation for the ratio of flame visible height to nozzle diameter has been given as [13]:

$$\frac{L}{D} = \frac{5.3}{C} \left[ C \frac{T_f}{AT_n} + (1-C) \frac{M_s}{M_n} \right]^{0.5} \quad (10)$$

As a boundary condition, the temperature of the elements adjacent to the flame is assumed equal to the adiabatic flame temperature.

As in Fig. 5 an element of the reaction tube wall with a length of  $\Delta Z$  has been considered. Considering different modes of heat transfer into the tube wall element, an energy balance can be set up [15].

$$\left( \text{Radiation from all elements of furnace walls and flame} \right) + \left( \text{Convection from combustion gas to tube elements} \right) \quad (11)$$

$$\left( \text{Heat transfer from tube skin to process fluid and catalyst} \right) + \left( \text{Radiation from combustion gas} \right) = 0$$

That is:

$$q_R + q_{conv} + q_{in} + q_{g-2} = 0 \quad (12)$$

$$q_{in} = U \cdot A_{in} \cdot (T_{pg} - T_w) \Delta Z \quad (13)$$

$$\frac{1}{U} = \frac{d_{ti}}{2\lambda} \ln \left( \frac{d_{te}}{d_{ti}} \right) + \frac{1}{\alpha} \quad (14)$$

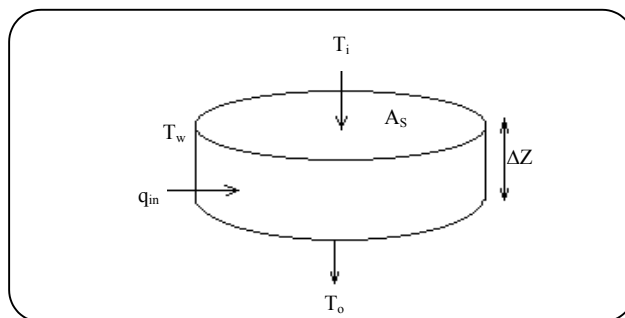


Fig. 6: Schematic diagram of an element of reaction medium inside the tube.

$\alpha$  is the convective heat transfer coefficient in the catalyst bed which is determined using correlations developed by Xu and Froment [7].

Similar to the furnace wall elements an electric analogy approach was used for radiation terms.

Fig. 6 shows a schematic diagram of an element of reaction medium inside the reactor tubes. An energy balance of heat transfer in the element is:

$$\left( \text{Energy transported by fluid} \right) + \left( \text{Energy transferred from tube skin} \right) + \quad (15)$$

$$\left( \text{Heat consumed by the chemical reactions} \right) = 0$$

That is:

$$UA_{in} \left( T_w - \frac{T_i + T_o}{2} \right) + (\rho_g C_p u_s A_s) (T_i - T_o) - \quad (16)$$

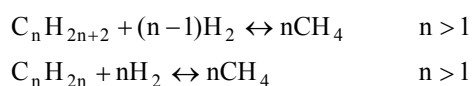
$$(\rho_B A_s \Delta Z) \left( \sum (\Delta H_i) r_i \eta_i \right) = 0$$

Energy balance for the element of combustion gases is in the form of:

$$\left( \text{Net heat transfer by radiation with all the surfaces} \right) + \left( \text{Heat transfer by convection with all the surfaces} \right) + \quad (17)$$

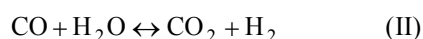
$$\left( \text{Energy released from combustion of fuel in the burners} \right) + \left( \text{Net energy transfer with the gas} \right) = 0$$

Methane-steam reforming reactions occur inside the reaction tubes. Small amount of heavier hydrocarbons convert to methane at the entrance of the reformer by exothermic hydrocracking reactions:



Studies show all of heavier hydrocarbons are converted to methane in the entrance zone of tubs.

The main reforming reactions occurring in the reactor are reforming (I), water gas shift (II) and methanation (III) reactions [16].



Form and constants of the intrinsic reaction rates are taken from the results of Xu and Froment [16].

$$r_1 = \quad (19)$$

$$\frac{k_1}{P_{H_2}^{2.5}} \frac{(P_{CH_4} P_{H_2O} - \frac{P_{H_2}^3 P_{CO}}{K_1})}{(1 + K_{CO} P_{CO} + K_{H_2} P_{H_2} + K_{CH_4} P_{CH_4} + K_{H_2O} P_{H_2O} / P_{H_2})^2}$$

$$r_2 =$$

$$\frac{k_2}{P_{H_2}} \frac{(P_{CO} P_{H_2O} - \frac{P_{H_2} P_{CO_2}}{K_2})}{(1 + K_{CO} P_{CO} + K_{H_2} P_{H_2} + K_{CH_4} P_{CH_4} + K_{H_2O} P_{H_2O} / P_{H_2})^2}$$

$$r_3 =$$

$$\frac{k_3}{P_{H_2}^{3.5}} \frac{(P_{CH_4} P_{H_2O}^2 - \frac{P_{H_2}^4 P_{CO_2}}{K_3})}{(1 + K_{CO} P_{CO} + K_{H_2} P_{H_2} + K_{CH_4} P_{CH_4} + K_{H_2O} P_{H_2O} / P_{H_2})^2}$$

Rate of formation of each component is:

$$r_{CO} = r_1 - r_2 \quad (20)$$

$$r_{CO_2} = r_2 + r_3$$

$$r_{CH_4} = r_1 + r_3$$

A one-dimensional heterogeneous model has been used for chemical reaction in the tubes. Continuity equations for  $CH_4$  and  $CO_2$  are:

$$\frac{dx_{CH_4}}{dz} = \frac{A_r \rho_B \eta_{CH_4} r_{CH_4}}{F_{CH_4}^\circ} \quad (21)$$

$$\frac{dx_{CO_2}}{dz} = \frac{A_r \rho_B \eta_{CO_2} r_{CO_2}}{F_{CH_4}^\circ}$$

Mass transfer resistance has a large effect on the catalyst performance, leading to effectiveness factors much less than unity. Transport resistances for each reaction have been taken into account by introducing effectiveness factor:

$$\eta_i = \frac{\int_0^V r_i P_s \rho_s \frac{dV}{V}}{r_i P_s^s \rho_s} \quad (22)$$

To find the profile of partial pressure of each component in the catalyst pellet, planar geometry can be used in solution of continuity equations for  $CH_4$  and  $CO_2$ . Since the gradients of partial pressure of all components are limited to a very thin layer near the surface, using planar geometry is justified for all catalyst shape. This is confirmed by checking the value of effectiveness factors for three reactions in equation (18). Parallel cross-linked pore model with uncorrelated pore size distribution and orientation has been used in evaluation of effective diffusivity of components in the catalyst pellet.

The effectiveness factors were calculated from equation (22) using orthogonal collocation method to calculate the concentration profile.

Pressure drop in the reactor is calculated by momentum equation:

$$-\frac{dP_t}{dz} = \frac{f \rho_g u_s^2}{gd_p} \quad (23)$$

Changes in physical properties of fluids have been considered [17-19].

## CATALYST SHAPE

In the reforming reaction, the catalyst should:

Make possible nearly full conversion of the hydrocarbon feed and a close approach to equilibrium for the methane steam reforming reaction at the reformer exit.

Maintain low tube wall temperature to ensure a long operation life. Cause a low and constant pressure drop.

To meet these requirements, the catalyst must have sufficient activity, resistance to carbon formation, mechanical strength and suitable shape [2]. Catalyst activity, resistance to coke formation and mechanical properties depend mainly on the particular catalyst formulation and preparation method. Although, for a given formulation decreasing catalyst size can increase the catalyst exposed area per unit reactor volume, one cannot reduce the catalyst particle size due to the pressure drop. With a given formulation, size and preparation method, catalyst shape is an important factor in achieving maximum activity for minimum pressure drop.

On the other hand in the steam-reforming reaction, the rate of the reactions is controlled not only by the kinetics of the reaction, but also by the rate of mass transfer from the bulk gas to the surface of the catalyst pellets and diffusion rates through the pores of the catalyst [1,7]. Studies show that the effectiveness factors of reaction are very small and in the order of  $10^{-2}$ . Concentration gradients inside the catalyst pellet are quite steep, with only the outer layer of the active material participating in the reaction catalyzing process. So at least 95% of the catalyst loaded into conventional reactor tubes is not utilized for catalyzing the reaction. Since only a thin layer of the catalyst is involved in the reaction, only the exposed surface of the catalyst pellet contains active metal and this is important parameter from economical point of view. Catalyst pellet of more complicated configuration, that give high internal surface area, low pressure drop and desired mechanical and hydrodynamic characteristics are desirable for this reaction and have been suggested.

So catalyst shape and intraparticle diffusion have considerable effect on reformer performance and must be considered.

The shape factor  $\phi_s$  of catalyst pellet is defined as:

$$\phi_s = \left( \frac{\text{surface of sphere}}{\text{surface of particle}} \right)_{\text{of same volume}} \quad (24)$$

Void fraction of the bed for each shape is estimated based on the catalysts shape factor [20]. Then the required tube length will be calculated. Hydrodynamic diameter for each shape is calculated from:

$$d_p = 6 \left( \frac{\text{pellet volume}}{\text{external surface of pellet}} \right) \quad (25)$$

More detail about modelling of catalyst shape effect have been presented by *Soltan Mohammadzadeh* and *Zamaniyan* [21].

## NUMERICAL SOLUTION

After setting up the governing equations of heat transfer and chemical reactions in the reactor furnace, the physical domains are discretized into a set of grids for numerical calculations. To reduce the number of equations, on the furnace wall, grids were generated on an area enclosing one burner. The whole length of a reaction tube has been discretized. Finite difference method was used to convert the first order heat conduction differential equations. The global spline orthogonal collocation method was used in solving the coupled differential continuity equation of key components ( $\text{CH}_4$  and  $\text{CO}_2$ ).

An iterative numerical method has been adopted for solving the set of simultaneous nonlinear equations. To initiate the calculations, seed values of temperature were assumed for the combustion gas in the furnace and grids on the furnace wall, tube skin and the process gas inside the reaction tubes. The initial composition of the reaction mixture and pressure distribution inside the tubes and physical properties were obtained. A system of  $M$  nonlinear equations and  $M$  unknowns was set up.

$$M = \left( \text{Number of wall elements} \right) + \left( \text{Number of combustion gas elements} \right) + \left( \text{Number of tube elements} \right) + \left( \text{Number of process gas elements} \right)$$

Newton method was used to solve the set of nonlinear equations to obtain new values for the temperatures and compositions. To obtain a reliable solution with a reasonable computation time, stability and convergence of the solution were checked by changing the grids size and initial values.

## SOFTWARE DEVELOPMENT

Using developed model, a windows based software has been developed for predicting reformer furnace performance. Fig. 7 Shows software main page with designed menus and icons. Input variable are summarized as:

-Furnace characteristics (including number of cells and rows, furnace dimension, number of burners and furnace walls to tubes distance)

- Tubes characteristics (including number of tubes, total tube length and heated tube length, inner and outer tube diameter, thermal conductivity and center to center tube distance)

- Feed characteristics (including composition, pressure and temperature)

- Combustion characteristics (including fuel type, oil or gas), fuel rate, composition, air characteristics, atomizing steam rate and its temperature)

- Catalyst characteristics (including type, dimension, solid density, thermal conductivity and porosity)

- Ambient characteristics (including temperature, pressure, air velocity and humidity)

- Insulation characteristics (including number of insulation layers and their thermal conductivity and thickness)

For inputting required data number of menu has been designed. Figs. 7 and 8 show some of these menus.

After inputting required data and running the program, the results can be studied from results menu. Output data are divided in two group:

- Graphs
- Specification sheets

In output results can be summarized as the following:

Physical properties of process gas and flue gas general, Product characteristics (composition, temperature and pressure).

Combustion characteristics (required air, fuel HHV and LHV, flue gas composition and rate, adiabatic flame temperature and heat released).

Process gas characteristics (profile of temperature, pressure, composition, rate of reactions, reaction effectiveness factors and component conversion versus tube length).

Furnace performance (heat released, heat adsorbed, tube skin temperature profile, max. temperature of tubes, outlet flue gas temperature, heat loss, weight and volume of catalyst, heat flux and surface exposed radiation).

## SOFTWARE CAPABILITIES

RIPI-RefSim software has some good capabilities. Some of software abilities are as following:

- Usable with SI & engineering system units
- Usable in rating, design and simulation modes
- Usable for syngas & hydrogen production units

(refinery, petrochemical, hydrogenation and iron ore reduction units)

- Facility of utilizing any feed gas
- Facility of utilizing any fuel oil & fuel gas
- Facility of exerting catalyst shape & properties effect
- Reports are available in standard specification sheets & as well as graphs (Figs. 9 and 10)
- Usable for process optimization (heat loss, cost, efficiency, life time, performance,...)
- Predicting of furnace performance in revamping cases(modification in furnace configuration, number of burners and tubes, feed, fuel, catalyst, insulation, ...)

## MODEL VERIFICATION

The performance of the model and developed software was verified by simulation of the performance of two terraced wall steam reforming furnace in the following Iranian refineries:

Tabriz refinery which is named as furnace 1.

Bandar abbas refinery which is named as furnace 2.

The main characteristics of the feed, catalyst and the furnace of furnace 1 and furnace 2 are summarized in table 1 and table 2 respectively.

In table 3 and table 4, results of the simulation run by developed software are compared with the measured values for furnace 1 and furnace 2, respectively. Good agreement between the measured and calculated values is an indication of good performance of the model and software. Consistent results of the parametric studies of the model proved its reliable performance [11].

Some of software results for furnace 2 which can be studied as graphs have been shown in Figs. 11 to 13.

## CATALYST SHAPE EFFECT AS A CASE STUDY

Assuming a constant mass of an industrial catalyst with different physical shapes, the performance of the reactor has been studied [21].

For comparison, in addition to the reference sphere, a cylinder, a single channel cylinder (ring), a multi-channel cylinder and a multi-channel cube have also been considered (refer to Fig. 14).

Since, using catalyst particles with the same volume but different shapes changes void fraction of the catalyst bed and length of the reaction tube, a fixed mass of catalyst has been taken as a basis.

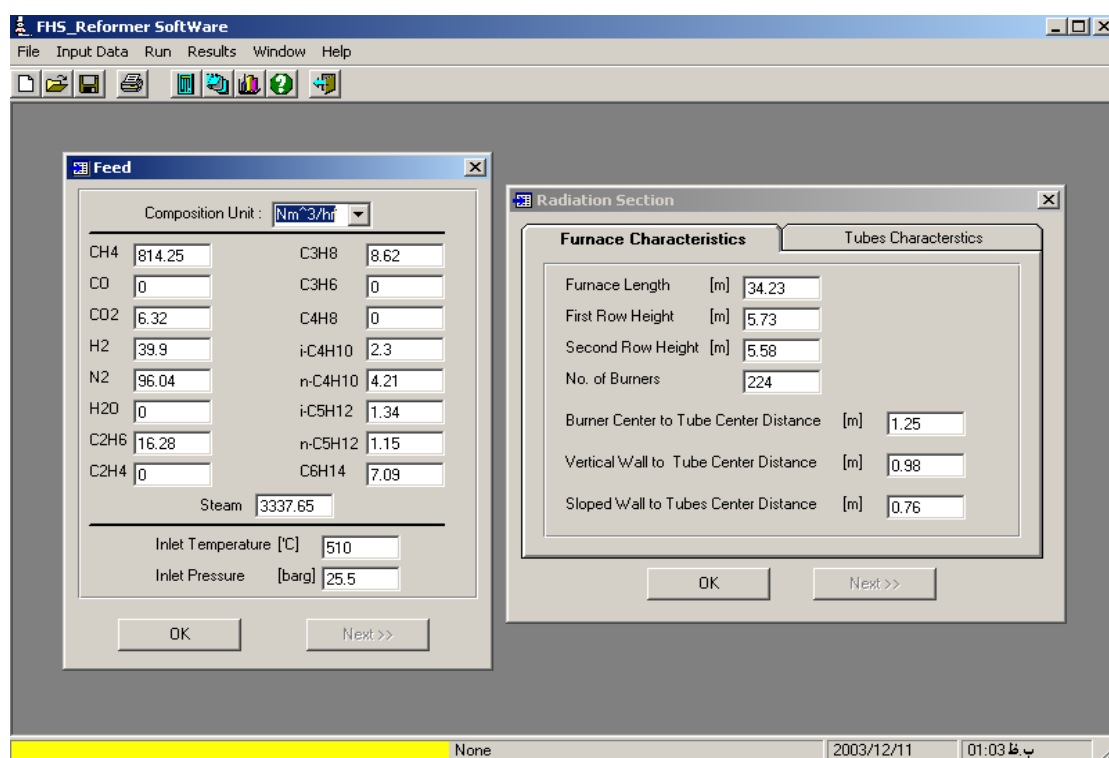


Fig. 7: Software main environment.

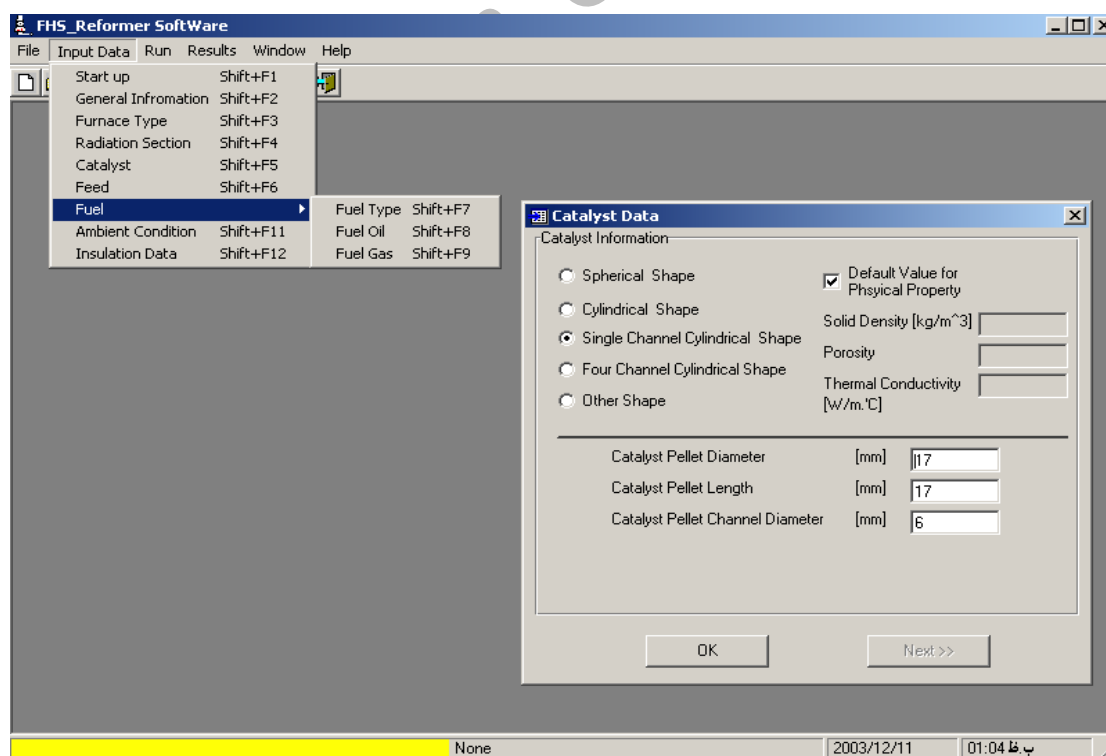


Fig. 8: Various input menus of software.



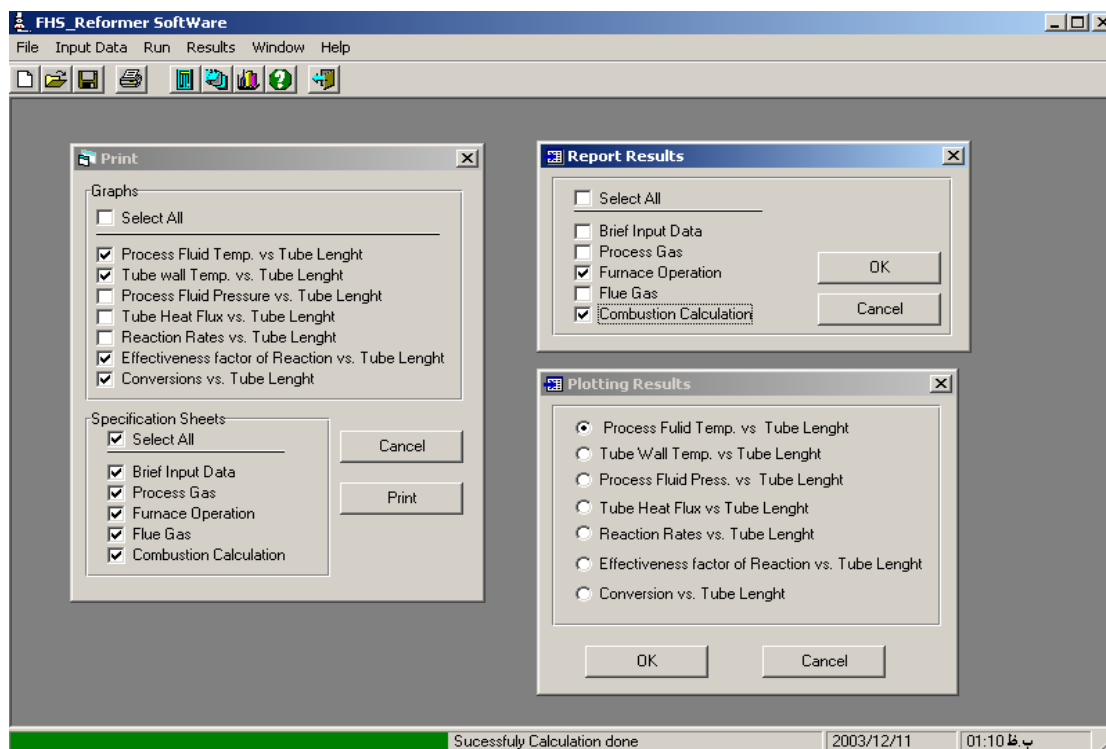










Fig. 9: Selection of ouput results in graphs and specification sheets type.

FHS\_Reformer SoftWare

File Input Data Run Results Window Help



1	<b>Reforemer Specification Sheet</b>				Job No. : Hydrogen	
2	Project Name : General Information				Reference No. : Hydrogen Production	
3	Address : 6954				Proposal No. : 0-345/23	
4	Plant Location : Test				Date Rev. : 582-548	
5	Service of Unit : 90-56/32				Item No. : 21/5/81	
6	Heater Type : Bandar Abbas				N.I.O.C Rev. : 58-631.25/4587	
7	Unit : Terraced Wall				Enquiry No. : 5847.25-6548	
8	Process Gas					
9	Inlet Condition					
10	Flow Rate [kg/hr]		Wet		Dry	
78281.1			18149.99			
11	Vapour Flow rate		Wet		Dry	
Nm <sup>3</sup> /hr			kmol/hr	Nm <sup>3</sup> /hr	kmol/hr	
97162.51			4335.15	22356.69	997.5	
12	Molecular Weight [kg/kmol]		18.06			
13	Outlet Conditions					
14	Temperature [°C]		1077.79			
15	Pressure [bar]		23.12			
16	Molecular Weight [kg/kmol]		12.56			
17	Flow Rate [kg/hr]		Wet		Dry	
78281.49			39899.58			
18			Wet		Dry	
Nm <sup>3</sup> /hr			kmol/hr	Nm <sup>3</sup> /hr	kmol/hr	
19						

Successfully Calculation done

2023/12/11

01:11

Fig. 10: A typical of software specification sheet.

Table 1: Characteristics of the feed, catalyst and the reformer reactor of furnace1.

Characteristics of the feed	
Temperature (K)	811.2
Pressure (bar)	21.5
Flow rate of gas per tube (Nm <sup>3</sup> /hr)	53.9
Flow rate of steam per tube (Nm <sup>3</sup> /hr)	405.1
Rate of equivalent CH <sub>4</sub> feed per tube (kmol/hr)	3.1
Feed molar ratio	H <sub>2</sub> O/CH <sub>4</sub> =5.48    CO <sub>2</sub> /CH <sub>4</sub> =0.16 H <sub>2</sub> /CH <sub>4</sub> =0.14    N <sub>2</sub> /CH <sub>4</sub> =0.01
Characteristics of the catalyst	
Catalyst type	Ni/MgO Al <sub>2</sub> O <sub>3</sub>
Mass of catalyst (kg)	18630
Shape	Ring shape
Dimensions (mm)	L(17) × ID(6) × OD(17)
Density( kg/m <sup>3</sup> )	2355.5
Thickness of active layer (mm)	2
Thermal conductivity (w/m.K)	8.6
Characteristics of the furnace	
Number of tubes	138
Number of burners	96
Tube ID (m)	0.124
Tube OD (m)	0.153
Total tube length (m)	13.31
Heated tube length (m)	11.74
H <sub>1</sub> (m)	4.95
H <sub>2</sub> (m)	4.71
H <sub>3</sub> (m)	1.56
θ (°)	84.35
Center to center tube distance (m)	0.22
Tube center to burner center distance (m)	1.25

To compare different shapes of catalyst pellet, a reference spherical shape has been considered. A number of catalyst particle shapes with the following properties have been considered [21] :

- Ease of manufacturing with conventional techniques
- Good mechanical strength
- High external surface area

A summary of the main characteristics of the reaction tubes and various catalyst shape have been given in table 5. Using the developed software, the effect of catalyst shape on some parameters has been studied and the results have been shown in Figs. 15 to 18.

## RESULTS AND DISCUSSION

Data on tube wall temperature profile is one of the most important factors in design and safe operation of a steam-reforming reactor. This data is useful in rating and determining the suitable material of construction for

reaction tubes at the design phase. During the operation, information on the maximum skin temperature, hot spot locations and points with a large thermal gradient and heat flux are crucial for a safe operation. Especially after a change in operating parameters or before implementing modification in reactor design or configuration it is important to evaluate their effect on reactor tube maximum temperature. Fig. 11 shows the skin temperature profile of a reaction tube and the reacting medium inside. It shows that there is a relatively constant temperature difference between the tube wall and the reaction fluid. At the length of about 6 m there is a distinct change in the uniform pattern mainly due to the second row of burners at this location.

Fig. 12 shows the rate of the three reactions in eq. (18), and the net rate of formation of CH<sub>4</sub>, CO and CO<sub>2</sub>. In the entrance zone of the reaction tube (i.e. Z<0.7 m), the endothermic effect of reaction (I) and (III) lowers the

Table 2: Characteristics of the feed, catalyst and the reformer reactor of furnace2.

Characteristics of the feed	
Temperature (K)	783.2
Pressure (bar)	25.5
Flow rate of gas per tube (Nm <sup>3</sup> /hr)	68.16
Flow rate of steam per tube (Nm <sup>3</sup> /hr)	228
Rate of equivalent CH <sub>4</sub> feed per tube (kmol/hr)	0.42
Feed molar ratio	H <sub>2</sub> O/CH <sub>4</sub> =3.5      CO <sub>2</sub> /CH <sub>4</sub> =0.007 H <sub>2</sub> /CH <sub>4</sub> =0.04      N <sub>2</sub> /CH <sub>4</sub> =0.1
Characteristics of the catalyst	
Catalyst type	Ni/MgO Al <sub>2</sub> O <sub>3</sub>
Mass of catalyst (kg)	29520
Shape	Ring shape
Dimensions (mm)	L(17) × ID(6) × OD(17)
Density (kg/m <sup>3</sup> )	2355.5
Thickness of active layer (mm)	2
Thermal conductivity (w/m.K)	8.6
Characteristics of the furnace	
Number of tubes	328
Number of burners	224
Tube ID (m)	0.098
Tube OD (m)	0.111
Total tube length (m)	-
Heated tube length (m)	13.6
H <sub>1</sub> (m)	5.73
H <sub>2</sub> (m)	5.58
H <sub>3</sub> (m)	1.45
θ (°)	85.1
Center to center tube distance (m)	0.2
Tube center to burner center distance (m)	1.25

reaction gas temperature, leading to a decrease in the net rate of reaction (I) and (III). In this region the rate of exothermic reaction (II) increases. Beyond this point, the rate of reaction (I) and (III) increases, although this increasing trend is flattened near the end of reactor. Although the temperature of reaction gas increases along the reaction tube, the gas composition approaches equilibrium, leading to decreasing reaction rate. The rate of reaction (II) shows a sign change at the reactor length of about 4 m. This indicates a change in the direction of this reaction.

Fig. 13 shows the effectiveness factor for the three reactions in equation (18) as a function of the reaction tube length. Generally the effectiveness factors of reaction (I) and (III) are less than 0.03 in the reactor. The effectiveness factors of both reaction (I) and (III) increase slightly near the entrance of the reaction tubes, then there

is a slightly decreasing trend. Effectiveness factor of the reaction (II) experiences a discontinuity at about 4 m of the tube length, due to the changing direction of the reaction.

A higher effectiveness factor translates to a more efficient use of a mass of catalyst. Effectiveness factor of reaction (I) has been plotted for the five shapes in Fig. 15. The general trends are the same for all shapes. The sphere has the lowest effectiveness factor while the multi-channel cube has the highest. Fig. 15 shows that the effectiveness factor of the sphere and cylinder fall into one category, while, single channel cylinder, multi-channel cylinder and multi-channel cube, fall into another category with higher effectiveness factor.

Pressure drop is a key parameter in the steam-reforming reactor. On the one hand, low pressure drop is a desirable characteristic of a particular catalyst shape,

**Table 3: Comparison of the model prediction with plant data of furnace 1.**

Parameter	Plant	Model	%Error
Reactor outlet temperature (K)	1117.2	1135.8	1.7
Reactor outlet pressure (kPa)	1925	1928	0.2
Maximum tube skin temperature (K)	1193.2	1208.6	1.3
Product flow rate (kgmol/hr)			
H <sub>2</sub>	10.58	10.66	0.8
CO	1.60	1.66	3.8
CO <sub>2</sub>	1.75	1.82	4.0
N <sub>2</sub>	0.02	0.02	0
CH <sub>4</sub>	0.26	0.25	3.8
H <sub>2</sub> O	12.97	12.48	3.8

**Table 4: Comparison of the model prediction with plant data of furnace 2.**

Parameter	Plant	Model	%Error
Reactor outlet temperature (K)	1133.2	1150.8	1.6
Reactor outlet pressure (kPa)	2350	2358	0.3
Maximum tube skin temperature (K)	1198.2	1213.6	1.3
Product flow rate per tube (kgmol/hr)			
H <sub>2</sub>	8.02	8.16	1.7
CO	1.41	1.47	4.2
CO <sub>2</sub>	1.0	1.05	5.0
N <sub>2</sub>	0.29	0.29	0
CH <sub>4</sub>	0.5	0.48	4.0
H <sub>2</sub> O	6.78	6.51	3.9
Heat absorption in radiation section (kJ/s)	65000	67345	3.6
Loss from furnace wall % of released	2.6	2.3	11.5
Flue gas temperature at the end of radiation section (K)	1268	1225	3.4
Fuel low heating value (kJ/kg)	41269	41360	0.2
fuel high heating value (kJ/kg)	45850	45765	0.2

**Table 5: Main characteristics of the various shapes of catalyst.**

Shape	Dimension	Shape factor, ( $\phi_s$ )	Void fraction, ( $\epsilon$ )	Tube length, L(m)
Sphere	D	1.0	0.37	7.50
Cylinder	H=D	0.8736	0.40	7.85
Single channel cylinder	H=D D=2d <sub>i</sub>	0.5769	0.60	11.77
Multi-channel cylinder (four channel)	H=D D=4d <sub>i</sub>	0.4555	0.65	13.46
Multi-channel cube (nine channel)	L=6d <sub>i</sub>	0.4051	0.70	15.70

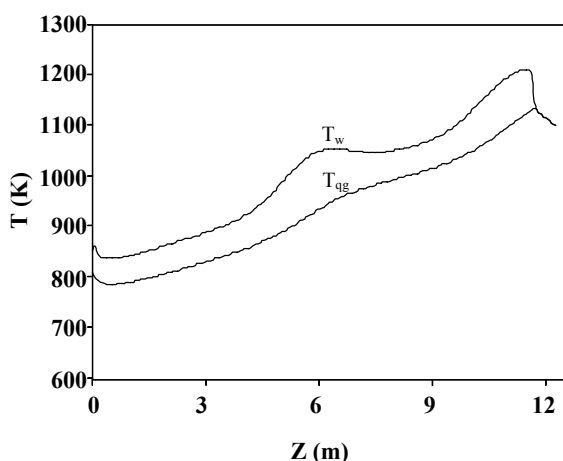


Fig. 11: Profile of tube skin temperature and process gas temperature.

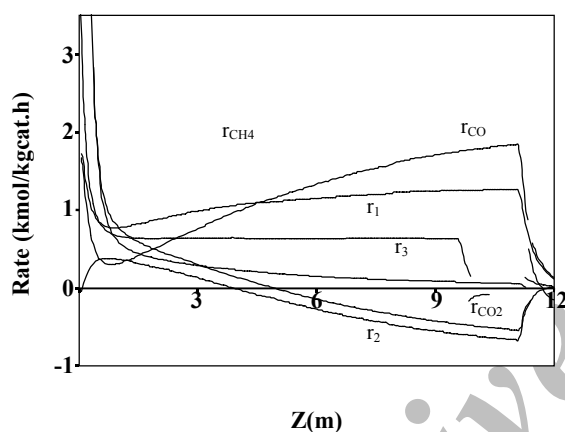


Fig. 12: Rate of the various reactions in equations (18) and (20) as a function of the tube length.

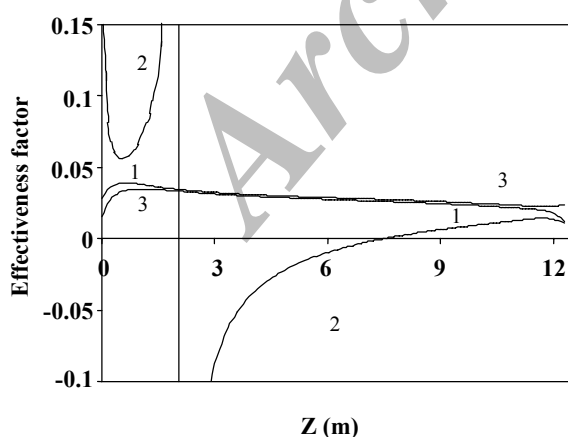


Fig. 13: Effectiveness factor of reactions in equation (18) as a function of the tube length.

because of a lower mechanical energy loss. On the other hand, high pressure drop indicates high turbulence and high heat transfer coefficient. High heat transfer coefficient, leads to a high reaction rate, a more active catalyst, lower reaction tube wall temperature and longer operation life of the tubes. Fig. 16 shows the distribution along the reaction tube for different shapes. Sphere and cylinder fall into the high pressure drop category, while the single and multi-channel cylinder and multi-channel cube fall into the low pressure drop category.

In Fig. 17 the temperature profiles of the reaction gas inside the tubes have been compared for different shapes along the reaction tube. The general trend shows a slight decrease in temperature, because of the cooling caused by the endothermic reactions. Then temperature increases monotonically, because of the decreasing of endothermic reactions' rate, decreased heat absorption and nearly constant heat flux. Fig. 17 shows that at any length of the reaction tube, the gas temperature is lower for multi-channel cube, multi-channel cylinder and single channel cylinder, while the temperature for sphere and cylinder is higher. For example at a length of 5 m, the difference in temperature for multi-channel cube and sphere is about 60 K. More active catalysts lead to lower gas temperature and lower tube skin temperature which increases reaction tube operating life span.

For a given mass of the catalyst but with different shapes, the conversion of  $\text{CH}_4$  at the reactor outlet is shown in Fig. 18. Sphere and cylinder shapes give a conversion of about 70%, while the highest conversion of about 85% is attainable with the multi-channel cube and a slightly lower conversion (cal. 83%) is obtainable with multi-channel cylinder. Single channel cylinder leads to a conversion of about 80%.

Considering the effect of catalyst shape on its pressure drop, heat transfer and kinetic characteristics, it seems that the multi-channel cube is the most desirable followed by the multi-channel cylinder, single channel cylinder, cylinder and finally sphere. In addition to these parameters, a desirable catalyst should be easy and practical to manufacture, handle and operate. It should also have good mechanical strength and attrition resistance. Considering these factors, the multi-channel cube has sharp edges, which can break and produce fines and particles, plugging the catalyst voids, leading to excessive pressure drop and uneven flow distribution.

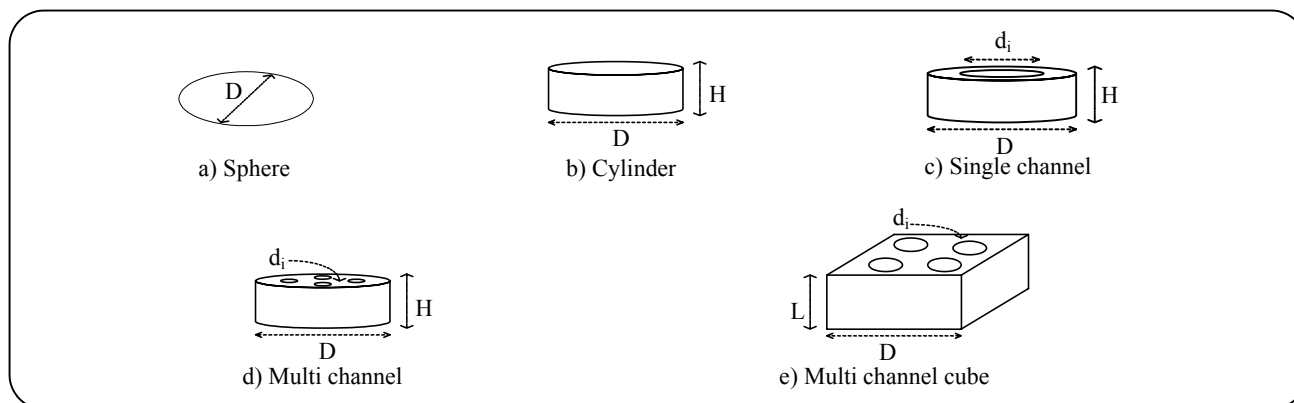


Fig. 14: Various shape of the catalysts.

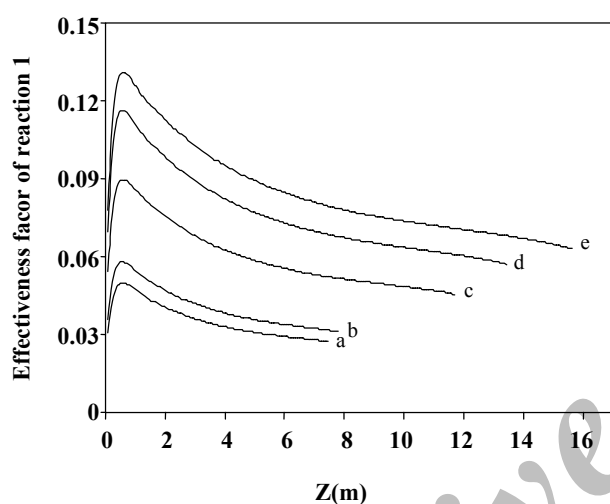


Fig. 15: Effectiveness factor of steam reforming reaction for different catalyst shapes.

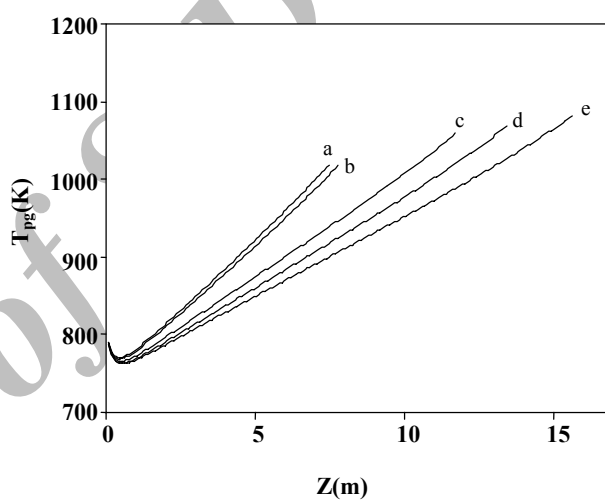


Fig. 17: Temperature profile of the process gas inside the reaction tubes for different catalyst shapes.

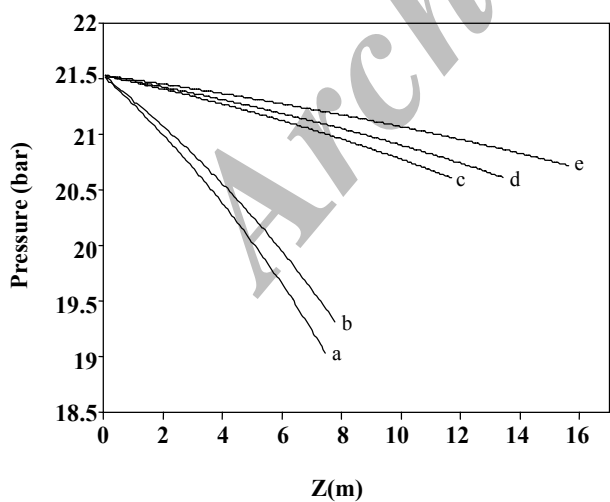
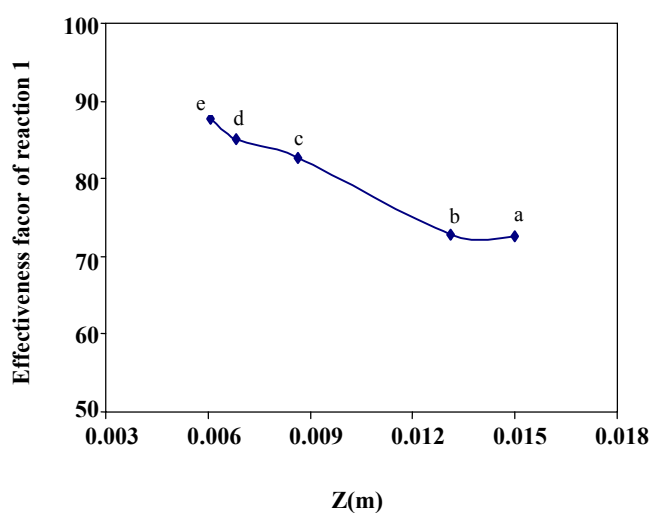


Fig. 16: Pressure profile along the tube for different catalyst shapes.

Fig. 18: Conversion of  $\text{CH}_4$  at the reactor outlet for different catalyst shapes.

These can cause hot spots, hot bands and hot tubes. Multi-channel cylinder and single channel cylinder seem to be the most suitable shapes. Comparing these two shapes, it seems that they have similar tendencies for attrition and fine production, while the multi-channel cylinder can have higher mechanical strength and lower tendency for breakage and particle formation.

## CONCLUSIONS

A User friend Windows base software has been developed for simulation of a catalytic reformer furnace. The reliability of the complete model has been verified by comparing its predictions with actual plant data. Using software, the effects of feed, fuel and catalyst characteristics, furnace configuration and insulation, and ambient condition, on furnace and reactor performance can be easily studied. For example as a case study, the effect of catalyst shape on performance of the reactor has been considered in developed mathematical model. Among different shapes of sphere, cylinder, single channel cylinder, multi-channel cylinder and multi-channel cube, the latter has the highest effectiveness, lowest pressure drop and lowest reaction gas temperature. Although the multi-channel cylinder is the second choice in terms of these parameters, it has better loading characteristics and higher attrition resistance.

## Nomenclature

A	Molar ratio of fuel to combustion products with theoretical air
$A_{in}$	Inner surface area of the tube element, ( $m^2$ )
$A_s$	Cross sectional area of the tube, ( $m^2$ )
$A_1$	Surface area of the furnace wall element, ( $m^2$ )
$A_2$	Outer surface area of the tube element, ( $m^2$ )
$C_p$	Heat capacity of process gas, ( $kJ.kg^{-1}.K^{-1}$ )
C	Molar ratio of fuel to mixture of fuel and air
D	Burner nozzle diameter, (m)
$d_p$	Hydrodynamic diameter of catalyst pellet, (m)
$d_e$	Tube external diameter, (m)
$d_i$	Tube internal diameter, (m)
$E_{b1}$	Black emissive power of the furnace wall element, ( $W.m^{-2}$ )
$E_{b2}$	Black emissive power of the tube wall element, ( $W.m^{-2}$ )
f	Friction factor in momentum equation
$F_{CH_4}^0$	Molar rate of methane in feed, ( $kmol.hr^{-1}$ )

$F_{12}$	Shape factor of the furnace wall element with respect to tube element
G	Acceleration of gravity, ( $m^2/hr$ )
$\Delta H_i$	Enthalpy of reaction "i", ( $kJ.kgmol^{-1}$ )
$J_1$	Radiosity of furnace wall element, ( $W.m^{-2}$ )
$k_i$	Reaction rate constant of reaction I
$K_i$	Adsorption constant of component I
L	Visible flame height, (m)
$M_n$	Molecular weight of fuel, ( $kg.kgmole^{-1}$ )
$M_s$	Molecular weight of surrounding gas, ( $kg.kgmole^{-1}$ )
N	Number of tubes
$P_i$	Partial pressure of component i, (kPa)
$P_{s,i}$	Partial pressure of component i on catalyst surface, (bar)
$P_t$	Total process gas pressure, (bar)
$q_{conv}$	Convection heat transfer between gas and surface, (W)
$q_{g-1}$	Radiation heat transfer between combustion gas and furnace wall element, (W)
$q_{g-2}$	Radiation heat transfer between combustion gas and tube wall element, (W)
$q_{in}$	Heat transfer from tube wall to process fluid, (W)
$q_{lost}$	Heat lost from furnace wall element to surroundings, (W)
$q_{m-1, n}$	Conduction heat transfer between element (m-1, n) and element (m,n) of the furnace wall, (W)
$q_R$	Radiation heat transfer between furnace elements and tube wall elements, (W)
$R_1$	Surface resistance of furnace wall element, ( $m^2$ )
$R_2$	Space resistance between furnace element and tube element, ( $m^2$ )
$R_3$	Surface resistance of tube element, ( $m^2$ )
$R_i$	Rate of reaction "i", ( $kgmol.kgcat^{-1}.h^{-1}$ )
$T_f$	Adiabatic flame temperature, (K)
$T_g$	Temperature of combustion gases, (K)
$T_i$	Temperature of process fluid entering a tube element, (K)
$T_{m,n}$	Temperature of furnace wall element, (K)
$T_n$	Fuel temperature at burner inlet, (K)
$T_o$	Temperature of process fluid leaving a tube element, (K)
$T_{pg}$	Temperature of process fluid, (K)

$T_w$	Temperature of external surface of tube wall element, (K)
$U$	Overall heat transfer coefficient, ( $\text{kJ.m}^{-2}.\text{h}^{-1}.\text{K}^{-1}$ )
$u_s$	Superficial velocity of process fluid, ( $\text{m}^3.\text{m}^{-2}.\text{h}^{-1}$ )
$X_i$	Conversion of component i
$\Delta x$	Length of furnace wall element in "x" direction, (m)
$\Delta y$	Length of furnace wall element in "y" direction, (m)
$z$	Reactor coordinate, (m)
$\Delta z$	Length of tube element, (m)

**Greek letters**

$\alpha$	Convective heat transfer coefficient in catalytic bed, ( $\text{kJ.m}^{-2}.\text{h}^{-1}.\text{K}^{-1}$ )
$\alpha_g$	Absorptivity of combustion gas
$\varepsilon_g$	Emissivity of combustion gas
$\varepsilon_r$	Emissivity of furnace wall
$\varepsilon_w$	Emissivity of tube wall
$\eta_i$	Effectiveness factor of reaction "i"
$\lambda$	Conductivity of tube, ( $\text{kJ.m}^{-1}.\text{h}^{-1}.\text{K}^{-1}$ )
$\rho_b$	Bulk density of catalytic bed, ( $\text{kg}_{\text{cat}}.\text{m}^{-3}_{\text{bed}}$ )
$\rho_g$	Density of gas, ( $\text{kg.m}^{-3}$ )
$\sigma$	Stephan-Boltzman constant, $=5.669 \text{ E-}8$ , ( $\text{W.m}^{-2}.\text{K}^{-4}$ )

Received : 1<sup>st</sup> June 2004 ; Accepted : 17<sup>th</sup> April 2006

**REFERENCES**

- [1] Adris, A. M., Pruden, B. B., Lim, C. J. and Grace, J. R., On Reported Attempts to Radically Improve the Performance of the Steam Methane Reforming Reactor, *Can. J. Chem. Eng.*, **74**, 177 (1996).
- [2] Rostrup-Nielsen, J.R., Christiansen, L.J. and Bak Hansen, J.H., Activity of Steam Reforming Catalysts: Role and Assessment, *Appl. Cat.*, **43**, 287 (1988).
- [3] Hyman, M., Simulate Methane Reformer Reactions, *Hydrocarbon Processing*, **47**, 131 (1968).
- [4] Davies, J. and Lihou, D., Optimal Design of Methane Steam Reformer, *Chem. Proc. Eng.*, **52**, 71 (1971).
- [5] Golebiowski, A. and Walas, T., Thermal Process in Catalytic Reforming of Methane with Water Vapor, *Int. Chem. Eng.*, **13**, 133 (1973).
- [6] Singh, C. P. P. and Saraf, D. N., Simulation of Side Fired Steam Hydrocarbon Reformers, *Ind. Eng. Chem. Process Des. Dev.*, **18** (1), (1979).
- [7] Xu, J. and Froment, G. F., Steam Reforming, Methanation and Water-Gas Shift Reaction :II- Diffusion Limitation and Reactor Simulation, *AIChE J.*, **35** (n1), 97 (1989).
- [8] Elnashaie, S. S. E. H., Adris, A. M., Soliman, M. A., Al-Ubaid, A. S., Digital Simulation of Industrial Steam Reformers for Natural Gas Using Hetrogeneous Models, *Can. J. Chem. Eng.*, **70**, 786 (1992).
- [9] Ferreira, R. M. Q., Marques, M. M., Babo, M. F., Rodrigues, A. E., Modeling of the Methane Steam Reforming Reactor with Large Pore Catalyst, *Chem. Eng. Sci.*, **47** (9-11), 2909 (1992).
- [10] Pedernera, M. N., Pina, J., Borio, D. O., Bucala, V., Use of a Hetrogeneous Two Dimensional Model to Improve the Primary Steam Reformer Performance, *Chemical Eng. J.*, **94**, 29 (2003).
- [11] Soltan Mohammadzadeh, J. S. and Zamaniyan, A., Simulation of Terraced Wall Methane Steam Reforming Reactors, *Iranian Journal of Science and Technology*, **26** (n B2), 249 (2002).
- [12] Rao, M. V. R., Plehiers, P. M. and Froment, G. F., The Coupled Simulation of Heat Transfer and Reaction in a Paralysis Furnace, *Chem. Eng. Sci.*, **43**(n6), 1223 (1988).
- [13] Kudo, K., Taniguchi, H. and Guo, K., Heat Transfer Simulation in a Furnace for Steam Reformer, *Heat Transfer Japanese Research*, **20** (n8), 750 (1992).
- [14] Holman, J.P., "Heat Transfer", Mc-Graw Hill Inc., New York, 319-542 (1992).
- [15] Hottle, H. C. and Sarofim, A. F., "Radiative Transfer", Mc-Graw Hill Inc., New York, (1967).
- [16] Xu, J. and Froment, G.F., Methane Steam Reforming, Methanation and Water-Gas Shift : I- Intrinsic Kinetics, *AIChE J.*, **35** (n1), 88 (1989).
- [17] Fogler, H. S., "Elements of Chemical Reaction Engineering", Prentice-Hall International Inc., Toronto, 607-660(1992).
- [18] Reid, R. C., Prausnitz, J. M., Poling, B. E., "The Properties of Gases & Liquids", McGraw-Hill, Toronto, 388-483 (1988).
- [19] Bird, R.B., Stewart, W.E., Lightfoot, E.N., "Transport Phenomena", John Wiley & Sons Inc., London, 793-797 (1966).



- [20] Kunii, D. and Levenspiel, O., "Fluidization Engineering", Butterworth-Hinemann, New York, 61-65 (1991).
- [21] Soltan Mohammadzadeh, J. S. and Zamaniyan, A., Catalyst Shape as a Design Parameter Optimum Shape for Methane Steam Reforming Catalyst, *Chemical Engineering Research and Design Journal*, **80**(n A), 383 (2002).

Archive of SID